

Effects of noise on leaky integrate-and-fire neuron models for neuromorphic computing applications

Thi Kim Thoa Thieu¹ and Roderick Melnik^{1,2}

¹ MS2Discovery Interdisciplinary Research Institute, Wilfrid Laurier University,
75 University Ave W, Waterloo, Ontario, Canada N2L 3C5

² BCAM - Basque Center for Applied Mathematics, Bilbao, Spain
{tthieu, rmelnik}@wlu.ca

Abstract. Artificial neural networks (ANNs) have been extensively used for the description of problems arising from biological systems and for constructing neuromorphic computing models. The third generation of ANNs, namely, spiking neural networks (SNNs), inspired by biological neurons enable a more realistic mimicry of the human brain. A large class of the problems from these domains is characterized by the necessity to deal with the combination of neurons, spikes and synapses via integrate-and-fire neuron models. Motivated by important applications of the integrate-and-fire of neurons in neuromorphic computing for biomedical studies, the main focus of the present work is on the analysis of the effects of random inputs on leaky integrate-and-fire (LIF) neuron models. One of the models examined here is based on a classical LIF model, while the other model is a LIF synaptic conductance neuron model. Our analysis is carried out via Langevin stochastic dynamics in a numerical setting describing cell membrane potentials. We provide the details of the models, as well as representative numerical examples, and discuss the effects of noise on the time evolution of the membrane potential as well as the spiking activities of neurons in both LIF models scrutinized here. Furthermore, our numerical results demonstrate that the presence of random inputs in LIF systems may substantially influence the spiking activities of neurons.

Keywords: ANNs · SNNs · LIF · Langevin stochastic models · neuromorphic computing · random input currents · synaptic conductances · neuron spiking activities · uncertainty factors · membrane and action potentials · neuron refractory periods

1 Introduction

In recent years, the modelling with artificial neural networks (ANNs) offers many challenging questions to some of the most advanced areas of science and technology [4]. The progress in ANNs has led to improvements in various cognitive tasks and tools for vision, language, behavior and so on. Moreover, some ANN

models together with the numerical algorithms bring the outcome achievements at the human-level performance. In general, biological neurons in the human brain transmit information by generating spikes. To improve the biological plausibility of the existing ANNs, spiking neural networks (SNNs) are known as the third generation of ANNs. SNNs play an important role in the modelling of important systems in neuroscience since SNNs more realistically mimic the activity of biological neurons by the combination of neurons and synapses [3]. In particular, neurons in the SNNs transmit information only when a membrane potential, i.e. an intrinsic quality of the neuron related to its membrane electrical charge, reaches a specific threshold value. The neuron fires, and generates a signal that travels to other neurons when the membrane reaches its threshold. Hence, a neuron that fires in a membrane potential model at the moment of threshold crossing is called a spiking neuron. Many models have been proposed to describe the spiking activities of neurons in different scenarios. One of the simplest models, providing a foundation for many neuromorphic applications, is a leaky integrate-and-fire (LIF) neuron model [13,17,18]. The LIF model mimics the dynamics of the cell membrane in the biological system [2,14] and provides a suitable compromise between complexity and analytical tractability when implemented for large neural networks. Recent works have demonstrated the importance of the LIF model that has become one of the most popular neuron models in neuromorphic computing [1,8,6,10,11,20]. However, ANNs are intensively computed and often deal with many challenges from severe accuracy degradation if the testing data is corrupted with noise [4,12], which may not be seen during training. Moreover, uncertainties coming from different sources [7], e.g. inputs, devices, chemical reactions, etc would need to be accounted for. To get closer to the real scenarios in biological systems as well as in their computational studies, we are interested in evaluating the contribution of uncertainty factors arising in LIF systems. In particular, the random inputs could influence the dynamics of LIF systems. A better understanding of random input factors in LIF models would allow for a more efficient usage of smart SNNs and/or ANNs systems in such fields as biomedicine and other applications [4,23].

Motivated by LIF models and their applications in SNNs and ANNs subjected to natural random factors in the description of biological systems, we develop LIF models of neuronal dynamics to study the effects of random external current inputs and random refractory periods on the spiking activities of neurons in cell membrane potential settings. In particular, one of the models that we consider is based on a classical LIF model, while the other considered model is a LIF synaptic conductance neuron model. Our analysis focuses on considering a Langevin stochastic equations in a numerical setting for a cell membrane potential with random inputs. We provide numerical examples and discuss the effects of random inputs on the time evolution of the membrane potential as well as the spiking activities of neurons in both models. Furthermore, we investigate the results of the classical LIF model with the data provided in [22], focusing on cortical pyramidal neurons (see, e.g., [23]). Finally, the second model of LIF

synaptic conductances is examined on the data from dynamic clamping (see, e.g., [14]) in the Poissonian input spike train setting.

2 Random factors and classical LIF models

2.1 SNN algorithm and model description

Let us recall the SNN algorithm, presented schematically in Fig. 1 (see, e.g., [6]). At the first step, pre-synaptic neuronal drivers provide the input voltage spikes. Then, we convert the input driver for spikes to a gently varying current signal proportional to the synaptic weights w_1 and w_2 . Next, the synaptic current response is summed into the input of LIF neuron N_3 . Then, the LIF neuron integrates the input current across a capacitor, which raises its potential. After that, N_3 resets immediately (i.e. loses stored charge) once the potential reaches/exceeds a threshold. Finally, every time N_3 reaches the threshold, a driver neuron D3 produces a spike.

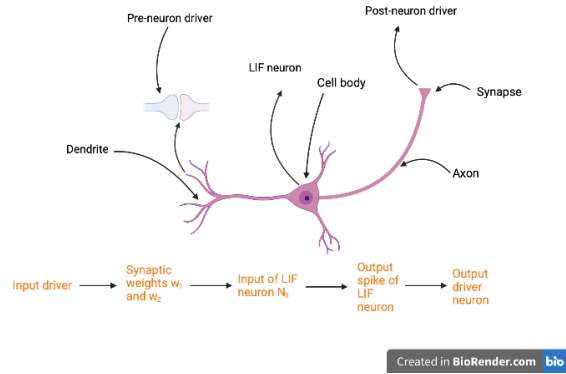


Fig. 1. [Color online] Sketch of SNN algorithm.

In general, the biological neuronal network is related to the SNN algorithm. Moreover, the main role of SNNs is to understand and mimic human brain functionalities since SNNs enable to approximate efficient learning and recognition tasks in neuro-biology. Hence, to have a better implementation of SNNs in hardware, it would be necessary to describe an efficient analog of the biological neuron. Therefore, in what follows, we are interested in the SNN algorithm starting from the third step, where the synaptic current response is summed into the input of LIF neuron, to the last step of the SNN algorithm. In particular, at the third step of SNN algorithm, it is assumed that the summation of synaptic current responses can be a constant, in a deterministic form or can be even represented by a random type of current. To get closer to the real scenarios

of neuronal models, we should also account for the existence of random fluctuations in the systems. Specifically, the random inputs arise primarily through sensory fluctuations, brainstem discharges and thermal energy (random fluctuations at a microscopic level, such as Brownian motions of ions). The stochasticity can arise even from the devices which are used for medical treatments, e.g. devices for injection currents into the neuronal systems. For simplicity, we consider a LIF model with random inputs of injection current and refractory period. A better understanding of the LIF model would assist in further improvements/developments of SNN implementations in hardware. In this section, we use the data provided in [22] to investigate our model.

In general, we know that the LIF model is equivalent to a model of an RC circuit [16]. In fact, in a cell membrane potential model, the insulator is not perfect. Indeed, the charge will, over time, slowly leak through the cell membrane [9]. The RC neuron response to an injected input current I_{inj} can be described by the following equation (see, e.g., [6]):

$$\tau_m \frac{d}{dt} V_m(t) = -(V_m(t) - E_L) + \frac{I_{\text{inj}}}{g_L} \quad \text{if } V(t) \leq V_{\text{th}}, \quad (1)$$

$$V_m(t) = V_{\text{reset}} \quad \text{otherwise}, \quad (2)$$

where V_m is the membrane potential, g_L is the leak conductance, E_L is the resting potential, I_{inj} is the external input current, while τ_m is the membrane time constant. In this model, we consider a random synaptic input by introducing the following random input current (additive noise) $I_{\text{inj}} = I_0 + \sigma_1 \eta(t)$, where η is the zero-mean Gaussian white noise with unit variance. For the multiplicative noise case, the applied current is set to $I_{\text{inj}} = I_0 + \sigma_2 V_m(t) \eta(t)$. Here, σ_1, σ_2 denote the standard deviations of these random components to the inputs. When considering such random input currents, the equation (1) can be considered as the following Langevin stochastic equation (see, e.g., [19]):

$$\tau_m \frac{d}{dt} V_m(t) = -(V_m(t) - E_L) + \begin{cases} \frac{1}{g_L} (I_0 + \sigma_1 \eta(t)) \\ \frac{1}{g_L} (I_0 + \sigma_2 V_m(t) \eta(t)) \end{cases} \quad \text{if } V(t) \leq V_{\text{th}}. \quad (3)$$

The LIF model (1)-(2) represents a neuron as a parallel combination of a “leaky” resistor (conductance g_L) and a capacitor (τ_m). The current source I_{inj} is used as synaptic current input to charge up the capacitor to produce potential $V(t)$, while V_{th} is the firing threshold, V_{reset} is the reset voltage, and E_L is the leak potential.

Based on (1)-(2), when potential exceeds threshold ($V(t) \geq V_{\text{th}}$), the capacitor discharges to a resting potential E_L using the voltage-controlled switch, like a biological neuron.

We know that there are three main events taking place during an action potential, namely, depolarization, repolarization and hyperpolarization. The action

potential frequency shows how often action potentials are sent. There exists a maximum frequency at which a single neuron can send action potentials, and this is determined by its refractory periods. Hence, the absolute refractory period is a time interval on the order of a few milliseconds during which a synaptic input will not lead to a second spike, see e.g. [16]. In the next section, we also investigate the effects of random refractory periods. We define the random refractory periods t_{ref} as $t_{\text{ref}} = \mu_{\text{ref}} + \sigma_{\text{ref}}\eta(t)$, where $\eta(t) \sim \mathcal{N}(0, 1)$.

2.2 Numerical results for a classical LIF model

We collect the sample mean of $N = 100$ realizations of the membrane potential $V(t)$ with random input currents of neurons. The sample mean and the sample variance at time $t \in [0, t_{\text{max}}]$ and for N realizations $V_n(t)$ are given by the following formulas

$$\langle V(t) \rangle = \frac{1}{N} \sum_{n=1}^N V_n(t) \quad (4)$$

and

$$\langle (V(t) - \langle V(t) \rangle)^2 \rangle = \frac{1}{N-1} \sum_{n=1}^N (V_n(t) - \langle V(t) \rangle)^2. \quad (5)$$

Following (1)-(2), we consider the membrane potential model where a spike takes place whenever $V(t)$ crosses V_{th} . In that case, a spike is recorded and $V(t)$ resets to V_{reset} value. This is summarized in the reset condition $V(t) = V_{\text{reset}}$ if $V(t) \geq V_{\text{th}}$.

The numerical results have been obtained by a discrete-time integration based on the Euler method implemented in Python.

In the simulations, we fix the parameters for $\tau_m = 30$ (ms), $E_L = -70$ (mV), $V_{\text{reset}} = -70$ (mV), $V_{\text{th}} = -50$ (mV), $g_L = 16.7$ (nS). These parameters have also been used in [22].

The main numerical results of our analysis are shown in Figs. 2-4. In the previous subsection, we have mentioned that the equation (1) can be consider as a Langevin stochastic equation by using random input current I_{inj} with additive and multiplicative noises. Hence, we have plotted the time evolution of the membrane potential, the spiking activity generated via 100 realizations of the Langevin stochastic processes (3) and the firing rates as described by our model. In our simulation, we use a standard electrophysiological technique, namely, the raster plot method that records the response of the neuron to each stimulus in membrane potential models.

In Fig. 2, we see the results obtained with model (1)-(2) with constant external current $I_{\text{inj}} = 3$ (mV). We also provide the results obtained with our model for different cases such as with constant refractory period and refractory period with noise. This classical LIF model has been studied earlier in [22], where the authors considered the model with the random injected current. In our model,

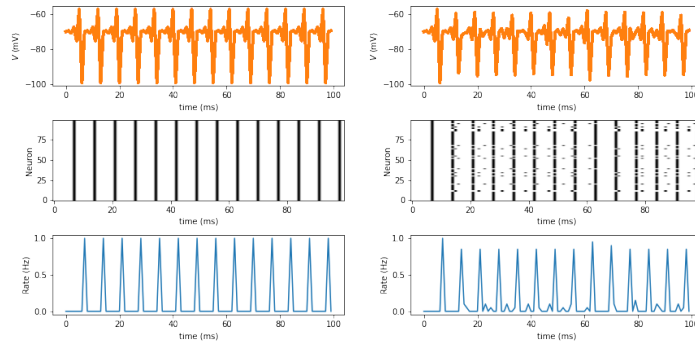


Fig. 2. [Color online] Top row: Average time evolution of membrane potential $V_m(t)$. Top left row: LIF deterministic model with $I_{inj} = 3$ (mV), $t_{ref} = 8$ (ms). Top right row: LIF model with $I_{inj} = 3$ (mV), $t_{ref} = \mu_{ref} + \sigma_{ref}\xi(t)$ (ms), where $\mu = 0$, $\sigma = 1$ and $\xi(t) \sim \mathcal{N}(0, 1)$. Middle row: the corresponding spiking activity generated via 100 realizations of the stochastic processes of the two cases of the top row. Bottom row: the corresponding firing rates of the two cases of the top row.

instead of considering only additive noise, we also investigate the effects of multiplicative noise in the system. In particular, we look at the first row of Fig. 2, where we plot the average time evolution of the membrane potential $V(t)$. We observe that the behavior of V is similar in the two cases. However, looking at the corresponding spiking activities of neurons, via a raster plots in the second row of Fig. 2, we observe the occurrence of fluctuations in the right panel of the second row in Fig. 2, while there are no such fluctuations in the deterministic case. Furthermore, the fluctuations occur also in the corresponding firing rate in the case with random refractory period input. The appearance of such fluctuations is due to the effect of random refractory period input. The numerical results in Fig. 2 show that the inter-trial variability is less than in the case studied in [22] (see Fig. 6A for comparison). This is due to the fact that we consider our model with constant injected current. We see that the constant input current makes the LIF model more stable with less variability compared to the case with random injected current. Moreover, the random refractory period could cause slight fluctuations in the system as seen in the second column of Fig. 2.

In Fig. 3, we provide the results of computations based on three modelling scenarios: when we use the model (1)-(2) with random external current $I_{inj} = 6 + 2\xi(t)$ (mV), and when we use this model for two different refractory period cases: with noise and without noise. In particular, looking at the left panel of the first row of Fig. 3, there is a strong fluctuation in the average time evolution of the membrane potential V compared to the deterministic case (top left panel) in Fig. 2. The average membrane potential decreases with value of $V = -66$ (mV) in the left panel of the first row in Fig. 3 compared to $V = -62$ (mV) in the deterministic case (top left panel) in the time interval [5;10] (ms) in Fig. 2. However, after time equal to 10 (ms), the spiking activity of neurons is reduced

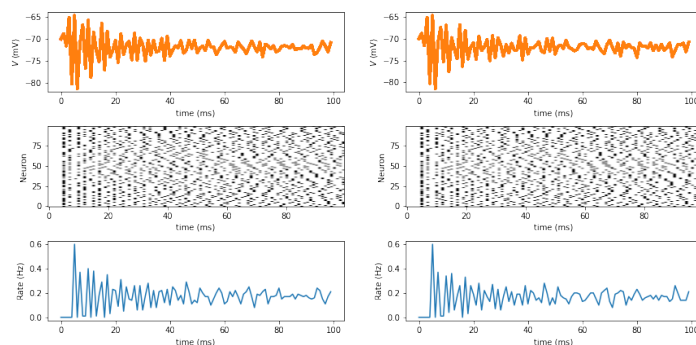


Fig. 3. [Color online] Top row: Average time evolution of membrane potential $V(t)$. Top left row: LIF model with $I_{inj} = 6 + 2\xi(t)$ (mV), $t_{ref} = 8$ (ms). Top right row: LIF model with $I_{inj} = 6 + 2\xi(t)$ (mV), $t_{ref} = \mu_{ref} + \sigma_{ref}\xi(t)$ (ms) and $\xi(t) \sim \mathcal{N}(0, 1)$. Middle row: the corresponding spiking activity generated via 100 realizations of the stochastic processes of the two cases of the top row. Bottom row: the corresponding firing rates of the two cases of the top row.

significantly with the value of V close to the value of V_{reset} . This is also visible in the left panel of the second row in Fig. 3, the raster plot shows a dramatical inter-trial variability when we inject a random input current in comparison to cases presented in Fig. 2. There is a significant decrease in the firing rate for the case presented in the bottom left panel of Fig. 3 compared with the case in the bottom left panel of Fig. 2. Furthermore, the random refractory period does not change much the time evolution of the membrane potential V , nor the spiking activity as described by our model in the case presented in Fig. 3. In the second column of Fig. 3, we add the random refractory period into the model. We see that the random refractory period does not change much the time evolution of the membrane potential V , the corresponding spiking activity and the firing rate. The firing rates in both cases in Fig. 3 are close to 0 after the time reaches 20 (ms). The raster plots show strong inter-trial variability in the cases of Fig. 3 compared with the cases presented in Fig. 2. It is clear that the presence of additive noise in the system affects the spiking activity of neurons. In order to prevent the changes in such neuronal spiking activities in SNNs and ANNs, we should try to reduce this additive noise in biological systems using the SNN algorithm.

We compare the first column of Fig. 4 with the second column of Fig. 3, when we increase the value of $\mu_{ref} = 5$ (ms). We see that the fluctuation is slightly reduced and the corresponding firing rate is close to 0 after the time reaches 10 (ms). However, in the top right panel of Fig. 4, when we inject a multiplicative noise type of random current $I_{inj} = 6 + 2V_m(t)\xi(t)$ (mV), the average membrane potential is reduced with the values smaller than $V_{reset} = -70$ (mV) compared to the cases of additive noise presented in Figs. 2-3. Furthermore, we analyze the corresponding spiking activity of the membrane potential in the middle right

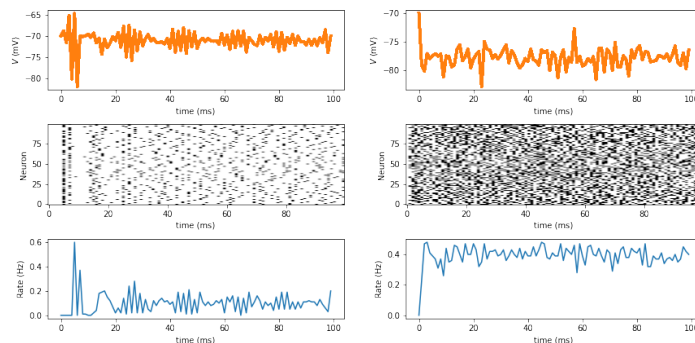


Fig. 4. [Color online] Top row: Average time evolution of membrane potential $V(t)$. Top left row: LIF model with $I_{inj} = 6 + 2\xi(t)$ (mV), $t_{ref} = \mu_{ref} + \sigma_{ref}\xi(t)$ (ms), where $\mu = 5$, $\sigma = 1$. Top right row: LIF model with $I_{inj} = 6 + 2V_m(t)\xi(t)$ (mV), $t_{ref} = \mu + \sigma\xi(t)$ (ms) and $\xi(t) \sim \mathcal{N}(0, 1)$. Middle row: the corresponding spiking activity generated via 100 realizations of the stochastic processes of the two cases of the top row. Bottom row: the corresponding firing rates of the two cases of the top row.

panel of Fig. 4. We observe that the spiking activity of neurons increases significantly compared to the previous cases with additive noise. The corresponding firing rate also increases dramatically from 0 to 0.4 (Hz). The raster plot in the second column of Fig. 4 shows that the presence of multiplicative noise in the system increases the inter-trial variability of the model compared with the case in Fig. 3. However, the variability in spiking activities of neurons in the presence of multiplicative noise is still less than in the case of additive noise. This is due to the fact that the firing rate in the case with multiplicative noise is larger than in the cases with additive noise. The presence of multiplicative noise also affects the spiking activities of neurons. This influence could lead to a decrease in spiking and firing activities of neurons in SNNs and/or ANNs systems.

3 A LIF synaptic conductance neuron model

We have demonstrated the importance of effects of random inputs on the classical LIF system. However, in biological systems such as brain networks, instead of physically joined neurons, a spike in the presynaptic cell causes a chemical, or a neurotransmitter, to be released into a small space between the neurons called the synaptic cleft [9]. Therefore, in what follows, we will focus on investigating chemical synaptic transmission and study how excitation and inhibition affect the patterns in the neurons' spiking output.

3.1 Model description: accounting for the LIF synaptic conductance neurons

In this section, we consider a model of synaptic conductance dynamics. In particular, neurons receive a myriad of excitatory and inhibitory synaptic inputs

at dendrites. To better understand the mechanisms of synaptic conductance dynamics, we investigate the dynamics of the random excitatory (E) and inhibitory inputs to a neuron via electrophysiological recording techniques [15].

In general, synaptic inputs are the combination of excitatory neurotransmitters. Such neurotransmitters depolarize the cell and drive it towards the spike threshold, while inhibitory neurotransmitters hyperpolarize it and drive it away from the spike threshold. These chemical factors cause specific ion channels on the postsynaptic neuron to open. Then, the results make a change in the neuron's conductance. Therefore, the current will flow in or out of the cell [9].

For simplicity, we define transmitter-activated ion channels as an explicitly time-dependent conductivity ($g_{\text{syn}}(t)$). Such conductance transients can be generated by the following equation (see, e.g., [5,9]):

$$\frac{dg_{\text{syn}}(t)}{dt} = -\bar{g}_{\text{syn}} \sum_k \delta(t - t_k) - \frac{g_{\text{syn}}(t)}{\tau_{\text{syn}}}, \quad (6)$$

where \bar{g}_{syn} (synaptic weight) is the maximum conductance elicited by each incoming spike, while τ_{syn} is the synaptic time constant and $\delta(\cdot)$ is the Dirac delta function. Note that the summation runs over all spikes received by the neuron at time t_k . Using Ohm's law, we have the following formula for converting conductance changes to the current:

$$I_{\text{syn}}(t) = g_{\text{syn}}(t)(V(t) - E_{\text{syn}}), \quad (7)$$

where E_{syn} represents the direction of current flow and the excitatory or inhibitory nature of the synapse.

In general, the total synaptic input current I_{syn} is the sum of both excitatory and inhibitory inputs. We assume that the total excitatory and inhibitory conductances received at time t are $g_E(t)$ and $g_I(t)$, and their corresponding reversal potentials are E_E and E_I , respectively. We define the total synaptic current by the following equation:

$$I_{\text{syn}}(V(t), t) = -g_E(t)(V - E_E) - g_I(t)(V - E_I). \quad (8)$$

Therefore, the corresponding membrane potential dynamics of the LIF neuron under synaptic current (see, e.g., [15]) can be described as follows:

$$\tau_m \frac{d}{dt} V(t) = -(V(t) - E_L) - \frac{g_E(t)}{g_L} (V(t) - E_E) - \frac{g_I(t)}{g_L} (V(t) - E_I) + \frac{I_{\text{inj}}}{g_L}, \quad (9)$$

where V is the membrane potential, I_{inj} is the external input current, while τ_m is the membrane time constant. Similar to the first model analyzed in Section 2, we consider here random synaptic inputs by introducing the following random input

current (additive noise) $I_{\text{inj}} = I_0 + \sigma_1 \eta(t)$, where η is the zero-mean Gaussian white noise with unit variance. In this representation, σ_1 denotes the standard deviation of this random component to the input. For the multiplicative noise case, the applied current is set to $I_{\text{inj}} = I_0 + \sigma_2 V(t) \eta(t)$, where σ_2 represents the standard deviation of this random components to the input. In what follows, we also consider the random refractory period as in the previous section. Similarly, in the presence of such random input currents, the equation (9) can be seen as a Langevin stochastic equation.

In our model, we use the simplest input spikes with Poisson process which provide a suitable approximation to stochastic neuronal firings [21]. This input spikes will be added in the quantity $\sum_k \delta(t-t_k)$ in the equation (6). In particular, the input spikes are given when every input spike arrives independently of other spikes. For designing a spike generator of spike train, let us call the probability of firing a spike within a short interval (see, e.g. [5]) $P(1 \text{ spike during } \Delta t) = r_j \Delta t$, where $j = e, i$ with r_e, r_i representing the instantaneous excitatory and inhibitory firing rates, respectively. This expression is designed to generate a Poisson spike train by first subdividing time into a group of short intervals through small time steps Δt . At each time step, we define a random variable x_{rand} with uniform distribution over the range between 0 and 1. Then, we compare this with the probability of firing a spike, which is described as follows:

$$\begin{cases} r_j \Delta t > x_{\text{rand}}, & \text{generate a spike,} \\ r_j \Delta t \leq x_{\text{rand}}, & \text{no spike is generated.} \end{cases} \quad (10)$$

3.2 Numerical results for the LIF synaptic conductance model

In this subsection, we take a single neuron at the dendrite and study how the neuron behaves when it is bombarded with both excitatory and inhibitory spike trains (see, e.g., [14,15]).

The simulations this section have been carried out by a modification of the numerical method provided in the open source framework at <https://github.com/W2D3/Biological-Neuron-Models-in-the-Neuromatch-Academy-directory>.

In the simulations, we choose the parameter set as follows: $E_E = 0$ (mV), $E_L = -60$ (mV), $E_I = -80$ (mV), $V_{\text{th}} = -55$ (mV), $V_{\text{reset}} = -70$ (mV), $\Delta t = 0.1$, $\tau_m = 10$ (ms), $r_e = 10$, $r_i = 20$, $n_E = 100$ spikes, $n_I = 50$ spikes. Here, n_E and n_I represent the number of excitatory and inhibitory presynaptic spike trains, respectively. These parameters have also been used in [14] for dynamic clamp experiments and we take them for our model validation. In this subsection, we use the excitatory and inhibitory conductances provided in Fig. 5 for all of our simulations. By setting the threshold to a very high value of $V_{\text{th}} = 1000$ (mV), we also investigate the time evolution of the free membrane potential in (9). Here, the free membrane potential means the membrane potential of the neuron when its spike threshold is removed.

The main numerical results of our analysis here are shown in Figs.6-8, where we have plotted the time evolution of the membrane potential calculated based

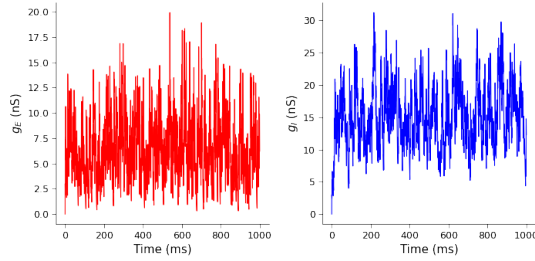


Fig. 5. [Color online] Left: Excitatory conductances profile. Right: Inhibitory conductances profile.

on model (9). We investigate the effects of random inputs on a LIF neuron under synaptic conductance dynamics. Under a Poissonian spike input, the random external current and random refractory period influence the spiking activity of a neuron in the cell membrane potential.

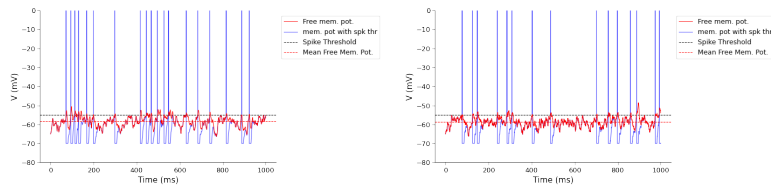


Fig. 6. [Color online] Time evolution of membrane potential $V_m(t)$. Left: LIF neuron under synaptic current with $I_{inj} = 8$ (mV), $t_{ref} = 8$ (ms), $g_L = 20$ (nS). Right: LIF neuron under synaptic current with $I_{inj} = 1 + 2\xi(t)$ (mV), $t_{ref} = 8$ (ms), $g_L = 20$ (nS), $\xi(t) \sim \mathcal{N}(0, 1)$.

In Fig. 6, we compare the results obtained with our model in two cases: the left plot with constant inputs for $I_{inj} = 8$ (mV) and $t_{ref} = 8$ (ms), the right plot with $I_{inj} = 1 + 2\xi(t)$ (mV), $t_{ref} = 8$ (ms). We observe that the time evolution of the free membrane and the membrane potential look similar in the two cases. There is a slight increase in the distance between each spike in the case with random input current I_{inj} .

In Fig. 7, in the left plot, when we consider both random input current I_{inj} and random refractory period t_{ref} , there is a long period of silence in the time evolution of the membrane potential from the time equal to 400 (ms) compared to the cases presented in Fig. 6. In the right plot of Fig. 7, the presence of multiplicative noise of injected current in the system causes bursting moods in the membrane potential and also in the free membrane potential case. However, when we increase the leak conductance from $g_L = 20$ (nS) to $g_L = 200$ (nS), the burst discharges are neglected in the case with multiplicative noise in Fig.

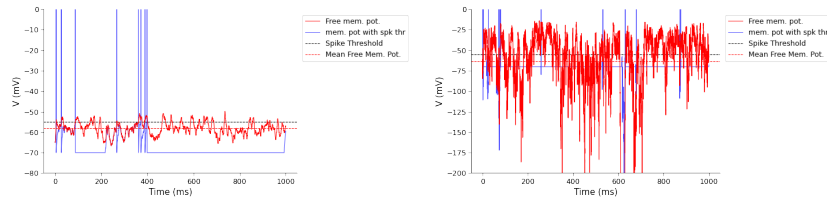


Fig. 7. [Color online] Time evolution of membrane potential $V_m(t)$. Left: LIF neuron under synaptic current with $I_{inj} = 1 + 2\xi(t)$ (mV), $t_{ref} = 1 + 2\xi(t)$ (ms), $g_L = 20$ (nS). Right: LIF neuron under synaptic current with $I_{inj} = 1 + 2V(t)\xi(t)$ (mV), $t_{ref} = 1 + 2\xi(t)$ (ms), $g_L = 20$ (nS), $\xi(t) \sim \mathcal{N}(0, 1)$.

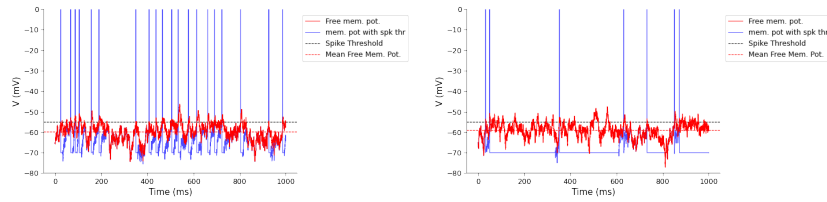


Fig. 8. [Color online] Time evolution of membrane potential $V_m(t)$. Left: LIF neuron under synaptic current with $I_{inj} = 1 + 2V(t)\xi(t)$ (mV), $t_{ref} = 8$ (ms), $g_L = 200$ (nS). Right: LIF neuron under synaptic current with $I_{inj} = 1 + 2V(t)\xi(t)$ (mV), $t_{ref} = 1 + 2\xi(t)$ (ms), $g_L = 200$ (nS), $\xi(t) \sim \mathcal{N}(0, 1)$.

8. In particular, in the left plot of Fig. 8, by considering the case of $I_{inj} = 1 + 2\xi(t)$ (mV) and $t_{ref} = 8$ (ms), we observe that the time evolution of the membrane potential looks quite similar to the case in the left panel of Fig. 6. However, we observe fluctuations in the membrane potential and also in the free membrane potential case. In the right plot of Fig. 8, for the case of both random (multiplicative noise) external current and random refractory period, there is an increase in the time interval between two nearest neighbor spikes similar to the case in the left plot of Fig. 7. We also observe fluctuations in the case in the right plot of Fig. 8.

Additionally, we notice that the presence of random refractory period increases the distance of the time interval between two nearest neighbor spikes. The presence of multiplicative noise causes burst discharges in the system. However, when we increase the value of leak conductance, the burst discharges are neglected.

Finally, we remark that noise may come from different sources, e.g., devices, environment, chemical reactions. Moreover, as such, noise is not always a problem for neurons, it can also bring benefits to nervous systems [7]. Managing such random factors in neural network models would allow for further improvements of smart SNN and/or ANN systems and an increased efficiency of neuromorphic computing in the fields of biomedicine and other applications.

4 Conclusion

We have proposed and described two LIF models with random inputs. In particular, we considered a classical LIF model as well as a LIF synaptic conductance model. Using the description based on Langevin stochastic dynamics in a numerical setting, we analyzed the effects of noise in the cell membrane potentials. Specifically, we provided details of the models along with representative numerical examples, and discussed the effects of random inputs on the time evolution of the cell membrane potentials, the corresponding spiking activities of neurons and the firing rates. Our numerical results have shown that the random inputs strongly effect the spiking activities of neurons in both LIF models. Furthermore, we observed that the presence of multiplicative noise causes burst discharges in the LIF synaptic conductance dynamics. However, when increasing the value of the leak conductance, the bursting moods are removed. Random inputs in LIF neurons could reduce the response of the neuron to each stimulus in SNNs and/or ANNs systems. A better understanding of uncertainty factors in neural network systems could contribute to further developments of SNN algorithms for higher-level brain-inspired functionality studies and other applications.

Acknowledgment

Authors are grateful to the NSERC and the CRC Program for their support. RM is also acknowledging support of the BERC 2022-2025 program and Spanish Ministry of Science, Innovation and Universities through the Agencia Estatal de Investigacion (AEI) BCAM Severo Ochoa excellence accreditation SEV-2017-0718 and the Basque Government fund AI in BCAM EXP. 2019/00432.

References

1. Brigner, W.H., Hu, X., Hassan, N., Jiang-Wei, L., Bennett, C.H., Garcia-Sanchez, F., Akinola, O., Pasquale, M., Marinella, M.J., Incorvia, J.A.C., Friedman, J.S.: Three artificial spintronic leaky integrate-and-fire neurons. *SPIN* 10(2), 2040003 (2020)
2. Cavallari, S., Panzeri, S., Mazzoni, A.: Comparison of the dynamics of neural interactions between current-based and conductance-based integrate-and-fire recurrent networks. *Front. Neural Circuits* 8(12) (2014)
3. Chen, X., Yajima, T., Inoue, I.H., Iizuka, T.: An ultra-compact leaky integrate-and-fire neuron with long and tunable time constant utilizing pseudo resistors for spiking neural networks. Accepted for publication in *Japanese Journal of Applied Physics* (2021)
4. Chowdhury, S.S., Lee, C., Roy, K.: Towards understanding the effect of leak in spiking neural networks. *Neurocomputing* 464, 83–94 (2021)
5. Dayan, P., Abbott, L.F.: *Theoretical Neuroscience*. The MIT Press Cambridge, Massachusetts London, England (2005)
6. Dutta, S., Kumar, V., Shukla, A., Mohapatra, N.R., Ganguly, U.: Leaky integrate and fire neuron by charge-discharge dynamics in floating-body mosfet. *Scientific Reports* 7(8257) (2017)

7. Faisal, A.D., Selen, L.P.J., Wolpert, D.M.: Noise in the nervous system. *Nature Reviews Neuroscience* 9, 292–303 (2008)
8. Fardet, T., Levina, A.: Simple models including energy and spike constraints reproduce complex activity patterns and metabolic disruptions. *PLoS Comput Biol* 16(12), e1008503 (2020)
9. Gerstner, W., Kistler, W.M., Naud, R., Paninski, L.: *Neuronal Dynamics: From single neurons to networks and models of cognition*. Cambridge University Press (2014)
10. Gerum, R.C., Schilling, A.: Integration of leaky-integrate-and-fire neurons in standard machine learning architectures to generate hybrid networks: A surrogate gradient approach. *Neural Computation* 33, 2827–2852 (2021)
11. Guo, T., Pan, K., Sun, B., Wei, L., Y., Zhou, Y.N., W, Y.A.: Adjustable leaky-integrate-and-fire neurons based on memristor coupled capacitors. *Materials Today Advances* 12(100192) (2021)
12. Hendrycks, D., Dietterich, T.: Benchmarking neural network robustness to common corruptions and perturbations. in: *International Conference on Learning* (2019)
13. Jaras, I., Harada, T., Orchard, M.E., Maldonado, P.E., Vergara, R.C.: Extending the integrate-and-fire model to account for metabolic dependencies. *Eur J Neurosci.* 54(3), 5249–5260 (2021)
14. Latimer, K.W., Rieke, F., Pillow, J.W.: Inferring synaptic inputs from spikes with a conductance-based neural encoding model. *eLife* 8(e47012) (2019)
15. Li, S., Liu, N., Yao, L., Zhang, X., Zhou, D., Cai, D.: Determination of effective synaptic conductances using somatic voltage clamp. *PLoS Comput Biol* 15(3), e1006871 (2019)
16. Mahdi, A., Ottesen, J.S.J.T., Olufsen, M.S.: Modeling the afferent dynamics of the baroreflex control system. *PLoS Comput Biol* 9(e1003384)
17. Nandakumar, S.R., Boybat, I., Gallo, M.L., Eleftheriou, E., Sebastian, A., Rajendran, B.: Experimental demonstration of supervised learning in spiking neural networks with phase change memory synapses. *Scientific Reports* 10(8080) (2020)
18. Pottelbergh, T.V., Drion, G., Sepulchre, R.: From biophysical to integrate-and-fire modeling. *Neural Computation* 33(3), 563–589 (2021)
19. Roberts, J.A., Friston, K.J., Breakspear, M.: Clinical applications of stochastic dynamic models of the brain, part i: A primer. *Biological Psychiatry: Cognitive Neuroscience and Neuroimaging* 2, 216–224 (2017)
20. Teeter, C., Iyer, R., Menon, V., Gouwens, N., Feng, D., Berg, J., Szafer, A., Cain, N., Zeng, H., Hawrylycz, M., Koch, C., Mihalas, S.: Generalized leaky integrate-and-fire models classify multiple neuron types. *Nature Communications* 9(709) (2018)
21. Teka, W., Marinov, T.M., Santamaria, F.: Neuronal integration of synaptic input in the fluctuation-driven regime. *The Journal of Neuroscience* 24(10), 2345–2356 (2004)
22. Teka, W., Marinov, T.M., Santamaria, F.: Neuronal spike timing adaptation described with a fractional leaky integrate-and-fire model. *PLoS Comput Biol* 10(3) (2014)
23. Woo, J., Kim, S.H., Han, K., M.: Characterization of dynamics and information processing of integrate-and-fire neuron models. *J. Phys. A: Math. Theor.* 54(445601) (2021)